Effect of Aftercooler Configuration on the Performance of Pulse Tube Cryocoolers

Y. Yasukawa[1], Y. Ueda[2]

[1] Fuji Electric Co., Ltd., Tokyo, Japan
[2] Tokyo University of Agriculture and Technology, Tokyo, Japan

ABSTRACT

This paper describes how the aftercooler configuration affects the performance of pulse tube cryocoolers. This is because the aftercooler is the main connection between the interior and exterior of the system. The convection heat transfer path in the aftercooler is gas passing near the outer casing via the heat exchanger body. It is important to enhance the convection heat transfer to reduce the thermal contact resistance. In this work, aftercoolers with various interior heat exchangers were constructed and their thermal characteristics were experimentally obtained using both steady flow and oscillatory flow. The experimental results show the difference between the thermal performances of the aftercoolers with the two flow types.

INTRODUCTION

The pulse tube cryocooler (PTC), which has no moving parts in the low-temperature side, is compact, highly reliable, and widely used for cooling sensors in consumer products, as well as in space applications[1-2]. Research on improving the performance of PTCs has been continuing via several methods. Operating at high frequency is a typical way to reduce the size and weight[3]. In pursuit of alternative methods, various studies have been conducted to improve the heat exchanger at the high-temperature side (aftercooler) and at the low-temperature side (cold head). The parallel plate type, in which the heat exchanger body is electro-discharge machined, is often used for the aftercooler, and fundamental research on the thermal characteristics of oscillatory flow on the plate-type heat exchangers has been carried out[4-6]. Because it is an integral structure, there is no concern for poor thermal contact between the parts. However, the amount of heat transfer is not sufficient, and it is possible that it cannot be improved. With the stacked copper screen that has been used conventionally for the heat exchanger body, the total heat transfer is sufficient, but thermal contact resistance exists at the boundary between the heat exchanger body and the outer casing, and it is not known whether the thermal contact resistance is sufficiently small. In this paper, we propose a symmetrical aftercooler configuration, measure the overall thermal resistance, and compare it to that of a conventional structure. Furthermore, we investigated the effect of the aftercooler configuration on the cooling performance by testing aftercoolers in both steady and oscillatory flows.

Cryocoolers 21, edited by R.G. Ross, Jr., J.R. Raab and S.D. Miller

HEAT TRANSFER PATH THROUGH AFTERCOOLER

The aftercooler has the important function of dissipating the heat, which is absorbed at the cold head and passes to the outside of the system through the regenerator. Figure 1 schematically shows the heat transfer path through the aftercooler, which consists of a heat exchanger body and outer casing. Based on the premise that the outside of the outer casing is cooled, heat is transferred in the following three consecutive paths: (1) Heat transfer between gas and the heat exchanger body by oscillatory flow, (2) Heat conduction through the heat exchanger body, and (3) Heat conduction (thermal contact resistance) between the heat exchanger body and the outer casing.

AFTERCOOLER CONFIGURATION

An aftercooler is composed of a heat exchanger body and an outer casing. Two configurations were prepared for the heat exchanger body by considering symmetry, as shown in Fig. 2. Type A is a conventional copper screen that is pressed and stacked into a copper cylinder and heat-treated (A1) or a silver-coated copper screen that is stacked and heat-treated (A2). Type A1 is made with a diffusion bond between the screen mesh and the outer casing, and A2 is brazed. The conditions of heat-treatment for A2 were determined by pre-testing the coating material, heating temperature, and holding time. For type B, a symmetrical multi-hole structure was formed by machining and was shrink fit into a copper cylinder. For type Bs,the aftercoolers were prepared with a flow straightener (FS), which is composed of fine screen meshes placed in front of the heat exchanger body.

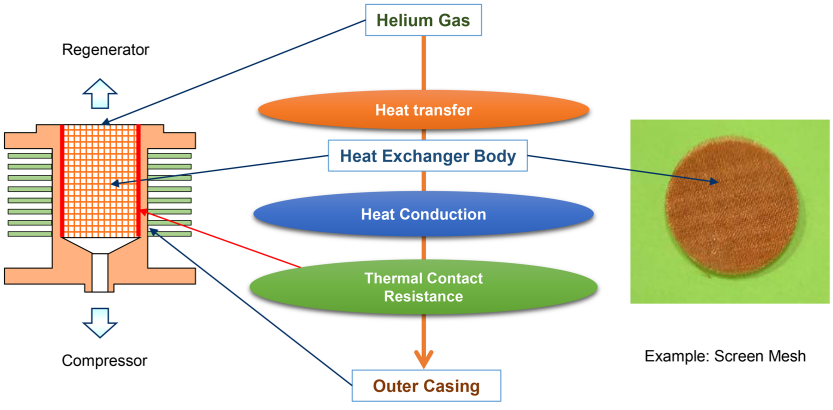

Figure 1. Components of an aftercooler and the heat transfer path

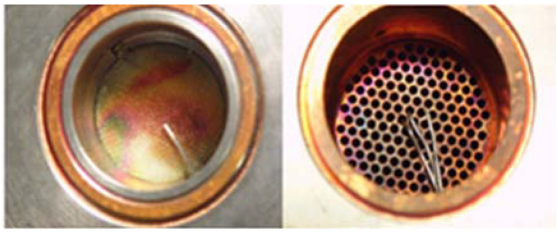

Figure 2. Aftercooler configurations
A: Stacked copper screen structure; B: Symmetrical multi-hole structure

EXPERIMENTAL SETUP

The performance of the aftercooler as a heat exchanger was tested under both steady and oscillatory flows. The experimental setup is basically the same as a conventional PTC except for the compressor and phase shifter, as shown in Fig. 3. Pressure and temperature sensors were carefully mounted in the aftercooler to prevent helium gas leakage. The test conditions – especially gas, pressure, and temperature – under steady flow were almost the same as those under oscillatory flow. During steady flow tests, the hot helium gas was supplied from the bottom of the PTC described on Fig. 3 (gas supplied not shown) through a direct connection to a gas cylinder. A valve placed at the outlet controls the pressure and flow, and the gas was finally released to the atmosphere.

The overall performance of the aftercooler was estimated by measuring the thermal resistance between the gas and the outer casing in the steady flow. Thermal resistance is an important parameter for comparing the performance of heat exchangers. Four and three measuring locations were specified for the gas and wall, respectively. To determine the thermal resistance, its representative temperature needs to be defined instead of the four or three measured temperatures. We determined the representative temperature as the surface integral average temperature obtained by curve fitting and integrating the measured temperatures.

EXPERIMENTAL RESULTS FOR STEADY FLOW

The experiment was carried out under the same conditions as the actual PTC operation as much as possible. Helium gas at around pressure of 2.0 MPa and a temperature of 20°C was used, but the flow rate was around one-tenth of the oscillating flow rate. The experimental results during the steady flow are shown in Fig. 4. The thermal resistance of type A1 is the largest, and the thermal resistance of type B, which has the symmetrical multi-hole structure without a FS, is the second largest.

Type A2 had improved thermal contact resistance between the heat exchanger body and the wall of the outer casing in comparison with type A1. This means that the silver coating on wires is effective for melting and connecting with the heat exchanger body and the wall inside the outer casing. The symmetrical multi-hole structure with the FS (Bs) showed the best performance.

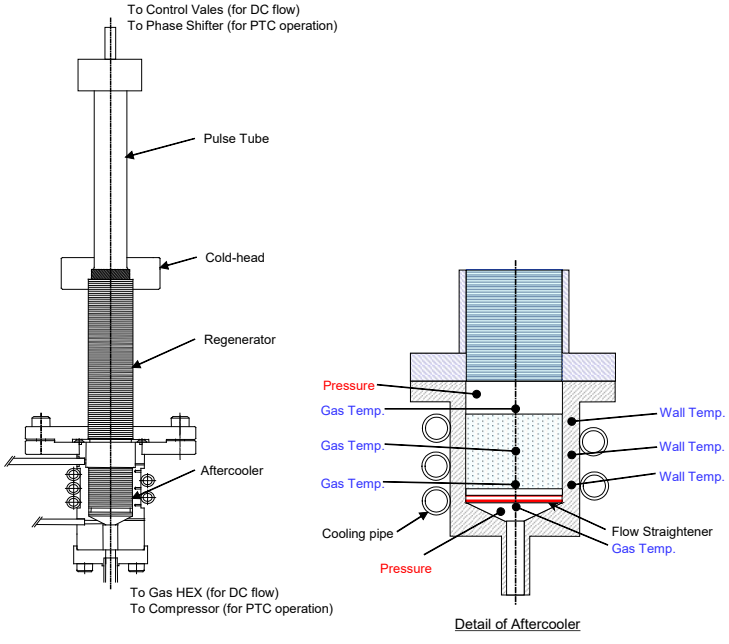

Figure 3. Schematic of the experimental setup

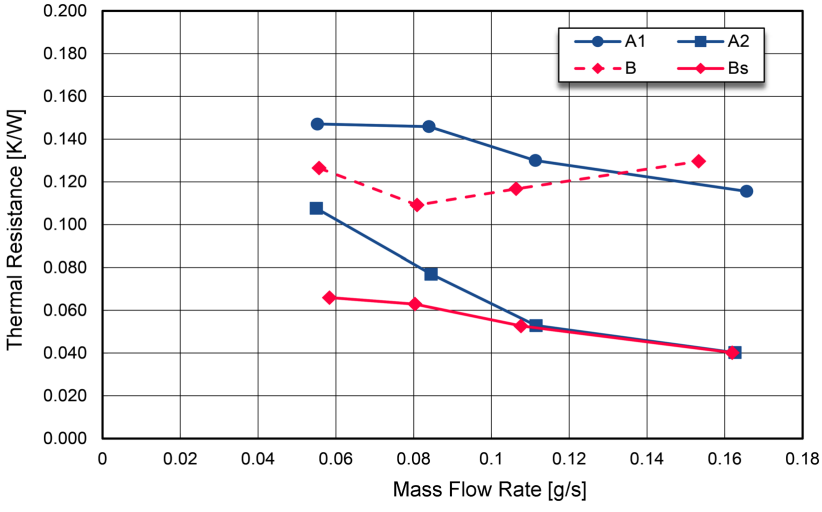

Figure 4. Thermal resistance measurement

COMPARISON OF THERMAL RESISTANCE

Heat transfer (path 1) by convection and heat conduction (path 2) can be calculated by a thermal circuit network. Unlike paths 1 and 2, the thermal contact resistance (path 3) is impossible to calculate. Thus, the calculation assumes that thermal contact resistance does not exist.

Figure 5 shows an outline of the calculation by the thermal network circuit model. The aftercooler configuration of both types A and B can be treated as axisymmetric. The heat exchanger body can be disassembled into cell units of gas and metal (copper) for calculation. Cell units of types A and B are also shown in Fig. 5. A metal cell and gas cell are connected by thermal conductance K_g, and

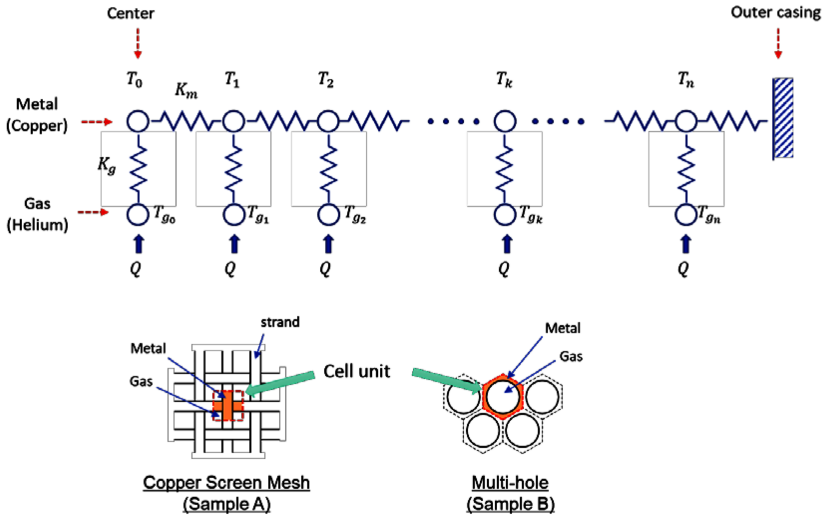

Figure 5. Schematic diagram of the model calculated by a thermal network circuit

the metal cell is connected to the adjacent metal cell by thermal conductance K_m. If the gas flows uniformly and the temperature distribution is uniform in the longitudinal direction, K_g and K_m are uniform and do not change under the same conditions, so the k-th temperatures of metal and gas are simply calculated as follows:

$$T_k = \sum_{i=k}^{n} i \cdot \frac{Q}{K_m} + T_w, \qquad K_m = \lambda \frac{A_m}{l}, \tag{1}$$

$$T_{g_k} = T_k + \frac{Q}{K_g}, \qquad K_g = hA_g, \tag{2}$$

where T_k is the temperature of the k-th metal unit, Q is the amount of heat exchange per unit time, T_w is the temperature of the outer casing, λ is the thermal conductivity of metal, A_m is the area of heat conduction per unit, l is the distance of heat conduction per unit, T_{gk} is the temperature of k-th gas unit, h is the convection heat transfer coefficient, and A_g is the area of the heat transfer per unit. Because the flow in both types A and B is laminar, the Nusselt numbers are calculated from Tanaka's formula[7] and the constant value associated with thermally-developed uniform wall heat flux[8].

The calculation was performed under the same conditions as the experiments, including no consideration of the thermal contact resistance between the heat exchanger body and the outer casing. The calculated gas temperature distributions are shown in Fig. 6. The temperature increase in the screen mesh of type A is smaller than that in the symmetrical multi-hole structure of type B. In these calculations, the temperatures at the edge point correspond with those of the outer casing in the experimental results. It can be seen that the temperature increase of type A at the edge is also smaller than that of type B. These results indicate a poor thermal contact between the heat exchanger body and the outer casing in type A. However, the temperature difference inside the body with an input heat of 42 W was 0.8 K for type A, while that for type B was 4.6 K, showing that type A intrinsically has potentially superior performance as a heat exchanger.

Figure 7 compares the experimental and calculated thermal resistance. The thermal resistance value was obtained from the calculation results by the same method as for the experimental results. In particular, the representative temperature was defined as the surface integral average temperature obtained by curve fitting. In type B (without FS), the calculations and experiments are in relatively good agreement. This is because the assumptions in the calculation are correct and the thermal

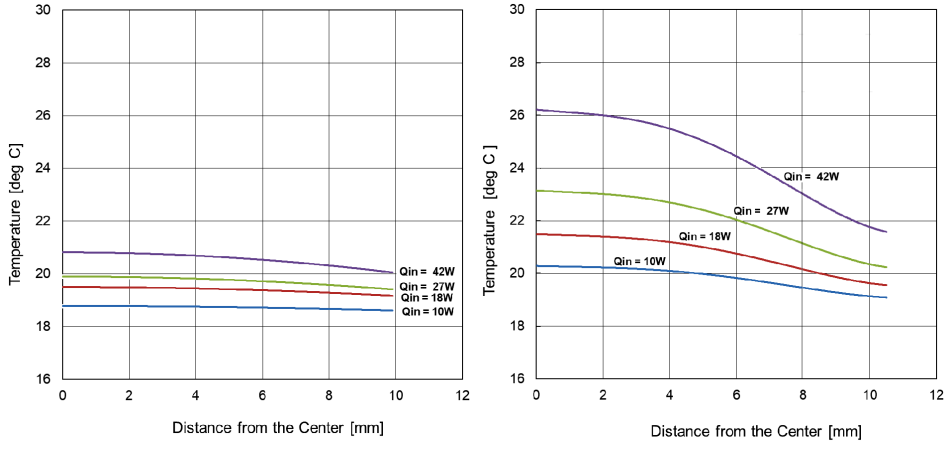

Figure 6. Calculation results for gas temperature (left: screen mesh, right: multi-hole structure)

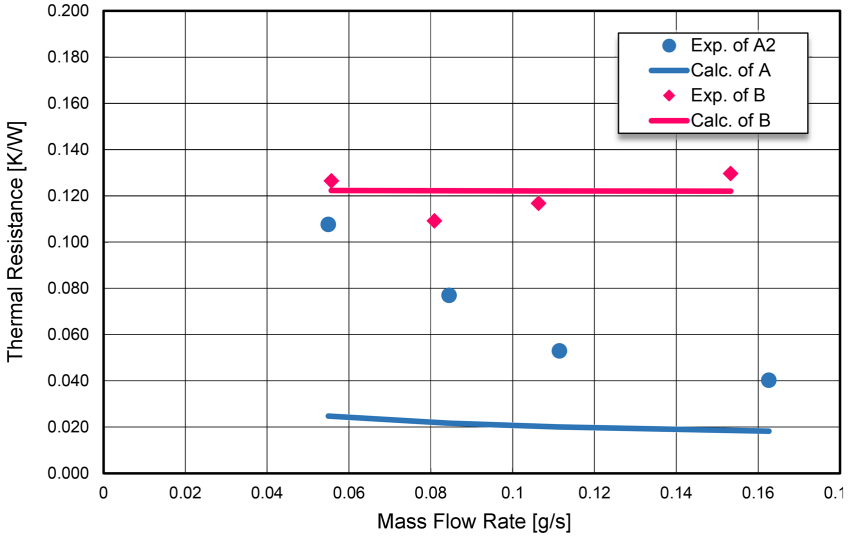

Figure 7. Thermal resistance comparison

contact resistance is negligible or sufficiently small. In type A, there is a difference between the calculations and experiments. Furthermore, the trend that the thermal resistance decreases as the flow rate increases can be seen in both the experiments and calculations. The difference between experiments and calculations is thought to be caused by the thermal contact resistance. The thermal resistance depends on the flow because the heat transfer efficiency increases as the flow rate in the screen mesh increases. On the contrary, the thermal resistance is almost constant as the flow rate increases in the symmetrical multi-hole structure. In the thermally-developed laminar flow with a uniform wall heat flux, the Nusselt number is a constant, which makes the heat transfer coefficient also a constant. This trend is the same in both the calculated and experimental values.

In the calculation, the thermal resistance due to heat transfer (path 1) and heat conduction (path 2) can be separately determined. Table 1 shows the calculation of the thermal resistance breakdown. The overall thermal resistance of the screen mesh is about one-seventh that of the multi-hole structure, and especially, the thermal resistance due to convection is about one-tenth.

EXPERIMENTAL RESULTS FOR OSCILLATORY FLOW

The aftercooler types were incorporated into a PTC, and cooler performance was evaluated. The main body of the PTC is shown in Fig. 4. The compressor used in this test had a structure with dual opposite pistons. Positions of both pistons were measured by linear variable differential transformers so that the flow rate could be obtained by time-differentiation of the piston position. Performance of the aftercooler was estimated by assessing the relation between the acoustic power versus no-load temperature. Acoustic power is calculated as shown in Fig. 8. Because the number

Table 1. Calculation of thermal resistance

	Screen Mesh (Sample A)	Symmetrical Multi-hole (Sample B)
(Path1) Heat Transfer	0.006 [K/W]	0.055 [K/W]
(Path2) Heat Conduction	0.012 [K/W]	0.067 [K/W]
Overall Thermal Resistance	0.018 [K/W]	0.122 [K/W]

of measurement points for pressure and flow rate was limited, the acoustic power was calculated from the measured values with some error included.

Figure 9 shows the test results of cooling performance in the oscillatory flow. The cooling performance was depicted by plotting the no-load temperature versus the acoustic power. The acoustic power W_1 is the horizontal axis in the figure. The symmetrical multi-hole structure without FS showed the best performance in spite of having the second-worst performance in steady flow.

On the contrary, type Bs (multi-hole structure with FS), which had the best performance with the steady flow, shows a performance equal to or less than that of type A. In this test, the temperatures of the gas and wall in the aftercoolers were also measured, as shown in Fig. 3. According to the results, a sharp gas temperature drop of 30 K or more is seen before and after the FS of type Bs.

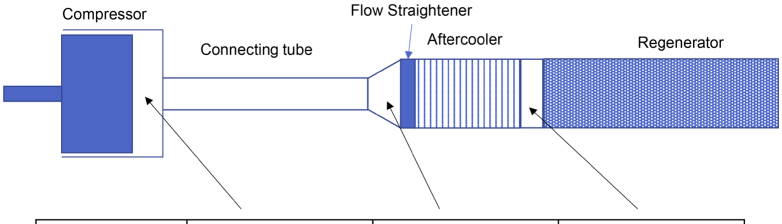

Position	0	1	2
Pressure	-	Measured (P_1)	Measured (P_2)
Flow Rate	Measured (U_0)	($U_1 \approx U_0$)	-
Acoustic Power	-	$W_1 = A_1 f \oint P_1 U_1 \, dt$	$W_2 = A_2 f \oint P_2 U_2 \, dt$

A: flow area, f: frequency

Figure 8. Schematic diagram of acoustic power assumption

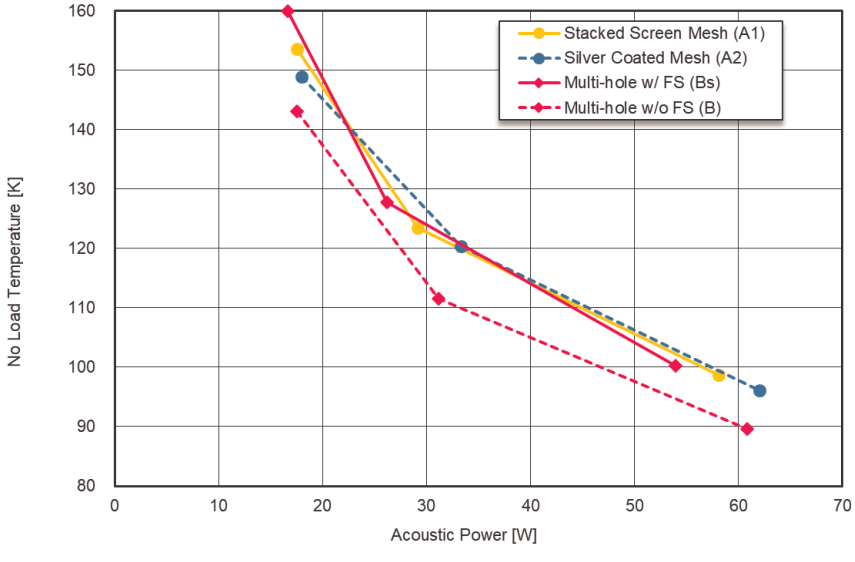

Figure 9. Acoustic power of W_1 (in front of AC) versus no-load temperature

DISCUSSION

In this experimental study, the cooling performance was evaluated for the acoustic power W_1, before the aftercooler (position 1 in Fig. 8). For comparison, the result of evaluating the acoustic power W_2 at position 2 using the flow rate of U_1 instead of U_2 and the cooling performance with respect to the acoustic power W_2 were not much different from that shown in Fig. 9.

The cause of the difference in the cooling performance with and without a FS is considered to be the fluid loss and the conversion of the work flow into heat flow in the FS. This is because the thermal contact between the FS and the outer casing was poor, meaning that the FS might have functioned like a regenerator.

In terms of the fluid loss, the difference can be confirmed by correct measurement of W_2 at position 2. If the flow rate and temperature according to the operating frequency can be measured, it is possible to determine whether work flow was converted to heat flow.

CONCLUSIONS

The steady flow in an aftercooler with a symmetrical multi-hole structure and a conventional copper screen was measured and evaluated as the performance of the heat exchanger. The symmetrical multi-hole aftercooler with a FS indicated the best overall performance in terms of the thermal resistance.

The cooling performance was assessed by incorporating each aftercooler separately into a PTC. The symmetrical multi-hole aftercooler without a FS had the best performance, contrary to the results for steady flow. Moreover, the factors that caused this difference were discussed.

As a next step, we will investigate and clarify the experimental results with an analysis based on the thermoacoustic theory.

REFERENCES

1. T. Koike, et.al, “Next generation hypernuclear γ-ray spectrometer: Hyperball-J”, the IX international conference on Hypernuclear and Strange Particle Physics (2007), pp.22-28
2. Y. Komiyama, et.al, “Hyper Suprime-Cam: Camera dewar design”, *Publications of the Astronomical Society of Japan*, (2018), 70 S2, pp. 1-39
3. S. Vanapalli, Z. Gan, R. Radebaugh, “120 Hz pulse tube cryocooler for fast cooldown to 50 K”, *Appl. Phys. Lett.* 90, 072504(2007), pp. 1-3
4. T. Ki, S. Jeong, “Optimal design of the pulse tube refrigerator with slit-type heat exchangers”, *Cryogenics vol.* 50(2010), pp. 608-614
5. K. Tang, J. Yu, T. Jin, Y.P. Wang, W.T. Tang, Z.H. Gan, “Heat transfer of laminar oscillating flow in finned heat exchanger of pulse tube refrigerator”, *Int’l Journal of Heat and Mass Transfer* 70(2014), pp. 811-818
6. X. Pang, W. Dai, X. Wang, S. Vanapalli, E. Luo, “Experimental study of the influence of cold heat exchanger geometry on the performance of a co-axial pulse tube cooler”, *Cryogenics vol.* 78(2016), pp. 78-82
7. M. Tanaka, I. Yamashita and F. Chisaka, “Flow and heat transfer characteristics of Stirling engine regenerator in oscillating", *Trans. JSME B* 55 (516), (1989), pp. 2478–2485
8. F. Incropera and D. DeWitt, *Fundamentals of Heat and Mass Transfer (5th ed.)*, (2002), pp. 486-487, ISBN 978-0-471-38650-6